

A Method for Eliminating Caprock Thickness Influence on Anomaly Intensities in Geochemical Surface Survey for Hydrocarbons

Liuping Zhang · Guoping Bai · Yingquan Zhao

Received: 29 March 2012 / Accepted: 16 July 2012 / Published online: 25 August 2012
© International Association for Mathematical Geosciences 2012

Abstract All petroliferous basins exhibit near-surface anomalous signals. The successful use of these signals must lead to great development in petroleum exploration. However, oil/gas fields cannot be effectively predicted in the case of intensive influence of caprock thickness on intensities of anomalies in a geochemical survey for hydrocarbons. In this paper, we first study the features of the influence of caprock thickness and then establish digital conceptual models for the influence in one and two dimensions. Finally, we develop techniques for eliminating this influence with wavelet analysis, based on the digital conceptual models. The newly developed techniques are applied to the actual data of acid-extractable hydrocarbons of soils in the southern slope of the Dongying Depression, East China where the anomaly intensities are considerably influenced by caprock thickness. The results illustrate that this new approach enables us to satisfactorily eliminate the influence of caprock thickness on anomaly intensities and thus can greatly improve the predictive capability of the existing geochemical data.

Keywords Geochemical exploration · Anomaly intensity · Caprock thickness · Wavelet analysis · Mallat wavelet

1 Introduction

Surface geochemical exploration for hydrocarbons dates back to 1929 when the first survey of this kind was carried out. Since then, this technique has been greatly

L. Zhang (✉) · Y. Zhao
Key Laboratory of Petroleum Resource, Institute of Geology and Geophysics, Chinese Academy of Science, Beijing 100029, China
e-mail: lpzhang@mail.iggcas.ac.cn

G. Bai
State Key Laboratory of Petroleum Resources and Prospecting, China University of Petroleum, Beijing 102249, P.R. China

modified and improved (Klusman 1993; Davidson 1994; Tedesco 1995). However, it is still considered to be an unconventional tool and has not frequently been used in present-day hydrocarbon exploration. Recent studies revealed the occurrence of hydrocarbon seepages in numerous basins (Burns et al. 2001; Wenger and Isaksen 2002; Sassen et al. 2003; Abrams 2005; O'Brien et al. 2005; Canet et al. 2006; Rollet et al. 2006; Sechman and Dzieniewicz 2007; Pinet et al. 2008; Loseth et al. 2009; Abrams and Dahdah 2010; Dembicki 2010; Logan et al. 2010; Mani et al. 2011; Sechman and Dzieniewicz 2011; Sechman et al. 2012). Furthermore, Abrams (2005) concluded that all petroliferous basins exhibit near-surface signals of hydrocarbon seepages. The successful use of these seepage signals must lead to great development in petroleum exploration. However, many geochemical signatures are not distinguishable from background signals with the methods currently used by industry. Relationships between near-surface hydrocarbon seepages and subsurface petroleum entrapment are often complex. Our research in the theory and application of surface geochemical survey has identified the problems in surface interference, multi-type anomalies and influence of caprock thickness on anomaly intensities. To improve surface geochemical prospecting, we have worked up a series of methods for interference elimination and anomaly recognition by using statistics, fractal geometry, wavelet analysis and artificial neural networks (Zhang 1993; Zhang and Liao 1998; Zhang and Bai 2002; Zhang et al. 2003, 2006). These methods were successfully used in many areas in China. However, the influence of caprock thickness on anomalous intensities has not been addressed, which has become a sticking point of surface geochemical prospecting where caprock is very thick or its thickness varies significantly. Logically, anomaly intensities decrease with burial depth. The caprock refers to a harder or more resistant rock formation with a very low permeability that may overlie oil or gas accumulations and prevent oil or gas from migrating to the surface. Therefore, caprock and its thickness play the most important role in reducing intensities of surface anomalies.

Over or near most oil pools where thick caprocks are present in the southern slope of the Dongying Depression in East China, there are no anomalies before and after the surface interference was eliminated. Therefore, the disappearance of the anomalies in contour maps does not result from surface interference. Our analyses indicate that the anomaly intensities can be largely reduced by thick caprocks so that they cannot be properly recognized or shown on contour maps. This illustrates that oil/gas pools cannot be correctly predicted by using surface geochemical survey if the influence of caprock thickness cannot be eliminated. Therefore, the influence of caprock thickness could be one of the many reasons why geochemical survey for hydrocarbons was not successful in some areas.

Wavelet analysis has been very successful in numerous scientific and engineering fields, especially in signal analysis and numerical applications (Li 1997; Zhang et al. 2003, 2006). Theories and methods of wavelet analysis and their development are documented in a number of publications including Pyrak-Nolte and Nolte (1995) and Li (1997). The multiresolution analysis (MRA) in wavelet analysis can extract information at various scales, providing a powerful tool for information analysis and processing. The detailed information in both space and frequency domains can be

simultaneously analyzed with wavelet analysis and can be accurately located and extracted. Most functions can act as mother wavelets. Wavelet analysis is, therefore, more flexible than Fourier analysis. Wavelet analysis has been applied to processing oxygen isotope data in marine sediments (Bolton et al. 1995), eliminating surface interference in geochemical hydrocarbon exploration (Zhang et al. 2003, 2006) and fracture detection from water saturation log data (Tokhmechi et al. 2009). The MRA makes it possible to apply wavelet analysis in more fields, probably including the elimination of the influence of caprock thickness on anomaly intensities.

Although anomaly intensities may be directly corrected with caprock thickness data from well-logging data, the amount of these data are usually not enough or are not available prior to extensive drilling where geochemical surveys might have been conducted. In addition, it is difficult or impossible to obtain a correction factor from caprock thickness data where several sets of caprock intervals occur. Therefore, a method has to be set up to extract information of caprock thickness influence from data of geochemical surface surveys. The method established in this paper was applied to the data in the southern slope of the Dongying Depression where the anomalies cannot be properly recognized or expressed on contour maps even though surface interference was eliminated. In the final results, the corrected anomalies coincide with oil pools (wells). It illustrates that the application of the newly established method can greatly improve the predictive capability of the existing geochemical data. Furthermore, we believe that our approach may be used to correct anomaly intensities whose variation is arisen from other geological influences that only change anomaly intensities.

2 Digital Conceptual Models for Eliminating Caprock Thickness Influence

The prerequisite to set up a method for the elimination of caprock thickness influence is to establish the digital conceptual models as they are required to test the feasibility of the method. For setting up the models, the geochemical background was set to be a constant into which Gauss noise ranging from 0 to 1 was added in order to make the model closely resemble real geochemical situations according to the study by Zhang et al. (2003). Previous studies (Klusman 1993; Ruan and Fei 1992; Tedesco 1995; Zhang 2003; Zhang et al. 2003, 2006) show that hydrocarbon anomalies are sharp peaks with a high-frequency variation, even in the case where the spacing is only 10 m between sampling points on the cross-section (Xu 1993). The digital conceptual model in one dimension was set up based on the noisy background and geometric feature of anomalies (Fig. 1).

In most geochemical surveys, there are both microseepage and seepage anomalies in geochemical data (Zhang 1993; Zhang and Liao 1998; Zhang and Bai 2002; Zhang et al. 2006). In some cases, there also exist macro-seepage anomalies. Macro-seepage usually refers to large concentrations of migrating hydrocarbons, which are generally visible and related to bulk flow (Zhang 1993; Abrams 2005). The seepage anomalies result from deep basin water and/or ultra-small gas bubbles migrating towards the surface along faults or unconformities (Zhang 1993; Zhang and Liao 1998; Zhang and Bai 2002; Zhang 2003). Microseepage anomalies are important for

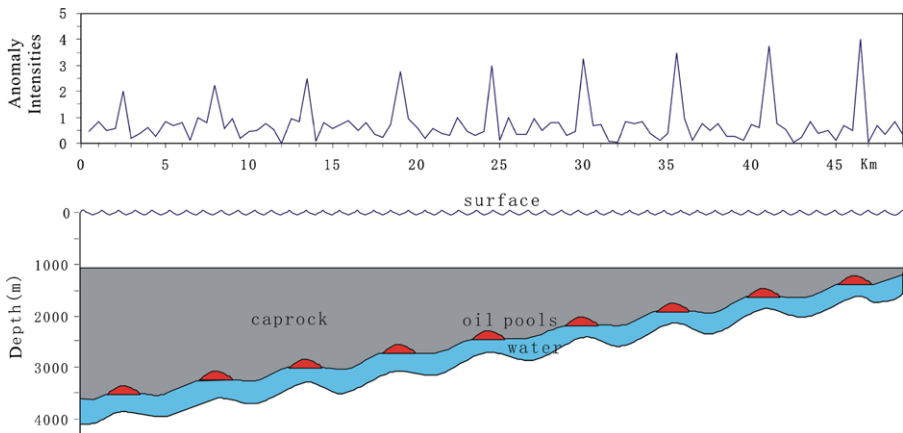


Fig. 1 1D Digital conceptual model for the influence of caprock thickness on intensities of microseepage anomalies

geochemical prospecting of hydrocarbon pools (Zhang 2003; Zhang et al. 2003, 2006) and formed via the microseepage mechanism (Price 1986; Zhang 1993; Klusman and Saeed 1996; Zhang and Liao 1998; Saunders et al. 1999; Brown 2000; Zhang and Bai 2002; Zhang 2003; Abrams 1992, 2005). This mechanism is described as the vertical ascent of ultra-small (colloidal-size) gas bubbles through a network of interconnected, groundwater-filled micro-fractures in caprocks (Price 1986; Zhang and Liao 1998; Zhang et al. 2003, 2006). According to this concept, bubble buoyancy drives them from oil/gas pools toward the surface in a near-vertical pathway (Fig. 1). As microseepage anomalies are formed from the gas ascent through caprocks and more developed than seepage anomalies in many cases (Zhang 1993; Zhang and Liao 1998; Zhang et al. 2003, 2006), the information of caprock thickness influence should be extracted from the variation of microseepage anomaly intensities. For this reason, seepage anomalies are not included in the model. Microseepage anomalies may be ring-shaped (Zhang 1993; Zhang and Liao 1998; Zhang and Bai 2002; Zhang et al. 2006). For convenience, we simplified them as anomaly points in the model.

The microseepage mechanism can be described with Darcy's law (Klusman 1993). The velocity of gas ascent is proportional to the multiplication product of caprock permeability and relative permeability of gas. For caprocks, permeability and relative permeability of gas are very low. Therefore, the migration velocity of gas bubbles is much lower in caprock layers than in the others. Thicker caprock constitutes a longer distance of gas bubble migration in the caprock. The longer migration at a low velocity, which goes with gas dispersion and adsorption, can result in the lower intensities of anomalies (Fig. 1).

The two-dimensional digital conceptual model was established on the base of the one-dimensional model. The two-dimensional background is still a constant into which Gauss noise arranging from 0 to 1 was added. Six lines with anomalies in Fig. 1 were added to the two-dimensional background. Figure 1 shows that 1.5 is the best value for separating anomalies from the background and that 0.5 can be used to

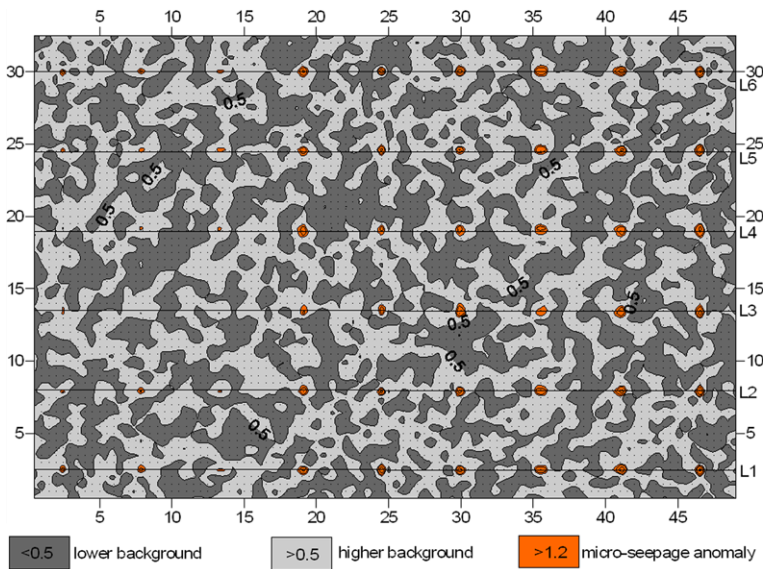


Fig. 2 2D digital conceptual model for the influence of caprock thickness on intensities of microseepage anomalies

divide lower and higher backgrounds. In order to more completely show anomalies, we use 1.2 as the lower limit of anomalies. In the two-dimensional model (Fig. 2), the sizes of anomalies decrease from right to left, corresponding to the variation of anomaly intensities in the one-dimensional model. It is noticeable that in the left part of Fig. 2, some low anomalies on low background cannot be shown by the contour of 1.2, even though we decreased the lower limit of anomalies. This illustrates that anomalies cannot be properly expressed on two-dimensional maps if the influence of caprock thickness cannot be eliminated. Under the conditions of more intense influence of caprock thickness, anomalies can disappear even in the one-dimensional map (traverse plot). Therefore, a method must be established to eliminate this kind of influence.

3 Development of Wavelet-Analysis-Based Techniques for Eliminating Caprock Thickness Influence

Mallat's wavelet is the derivation of its mother wavelet (the cubic spline) that is a smoothing function close to the Gaussian function (Mallat and Zhong 1992). It is anti-symmetrical, regular, and has a small compact support. These properties of Mallat's wavelet ensure the reliability and accuracy of wavelet analysis, avoid irregular displacement and addition of high-frequency information when MRA is conducted, and make low-pass information smoothing and successive in MRA. Therefore, it has been successfully used in edge detection (Mallat and Zhong 1992), contour analysis in the image-processing field (Palacios et al. 2011) and interference elimination

in surface geochemical exploration (Zhang et al. 2003, 2006). Due to these advantages, Mallat's wavelet is employed to develop the method for eliminating influence of caprock thickness in surface geochemical exploration.

The variation of caprock thickness presents low-frequency information and thus results in the influence of low-frequency information on geochemical data. But it only affects anomalies that exist in high-frequency information (refer to Zhang et al. 2003, 2006), as shown in Fig. 1. To obtain the low-frequency information reflected by anomalies, pre-processing of anomaly data for wavelet analysis is needed. Firstly, anomalies are broadened according to the scales at which surface interference is eliminated. The anomaly broadening decreases the frequency of anomaly variation and thus can help to take low-frequency information reflecting caprock thickness influence. The broadened widths (numbers of data points) of anomalies are restricted and should be close to or less than $2^{\text{scales}} + 1$. Otherwise, the variation frequency of broadened anomalies may become too low to represent the low frequency of variation of original anomaly intensities. Secondly, the broadened anomalies and their locations are used for the interpolation and extrapolation for the values at the other locations. Although the anomalies without broadening can be directly used to interpolate and extrapolate for the values of chemical variables at the other locations, these interpolation and extrapolation may cause aberrance, especially in margins, when anomalous points are relatively few or distributed unevenly. This is another reason why anomalies need to be broadened. The influence of caprock thickness belongs to multiplication type. Therefore, logarithms of the data of the digital model are taken. Then according to the properties of wavelets, the normalization (Eq. (1) in Zhang et al. 2003) of these logarithmic data was performed before wavelet analysis. In wavelet analysis, the data at the border may singularly vary if the border is not treated. Therefore, symmetric border treatment is used in this study, on the basis of the geometric features of anomalies and influence of caprock thickness as shown in Fig. 1.

The one-dimensional wavelet analysis of the pre-processed data is shown in Fig. 3. Scale 3 is often used in surface interference elimination (Zhang et al. 2003, 2006). To eliminate the influence of caprock thickness in the one-dimensional model, we use the same scale as surface interference elimination, because at this scale, the unnecessary variation of the anomalies after surface interference elimination will not arise from extraction of low-frequency information of caprock thickness influence. The anomaly widths (seven points) of the sequence C0 (the pre-processed data) in Fig. 3A are less than $2^3 + 1$. As shown in Fig. 3A, the continuous sequence at scale 3 (C3) can exactly reflect the low-frequency information of the anomalies shown in Fig. 1, although anomaly broadening imported high-frequency information shown by the detailed sequences (D1–D3) in Fig. 3B. We let detailed sequences D1–D3 in Fig. 3B equal to zero and conducted inverse wavelet transform using the sequence C3. In this way, the low-frequency information reflected by C3 was taken and the high-frequency information imported from anomaly broadening was removed. Then, we performed inverse log-normalization of the low-pass filtering data and got the information of the variation of anomaly intensities (LP in Fig. 3C). Here we introduce the concept of the correction factor to eliminate the influence of caprock thickness

$$F_i = \frac{\sum_{j=1}^n LP_j}{n \cdot LP_i}, \quad (1)$$

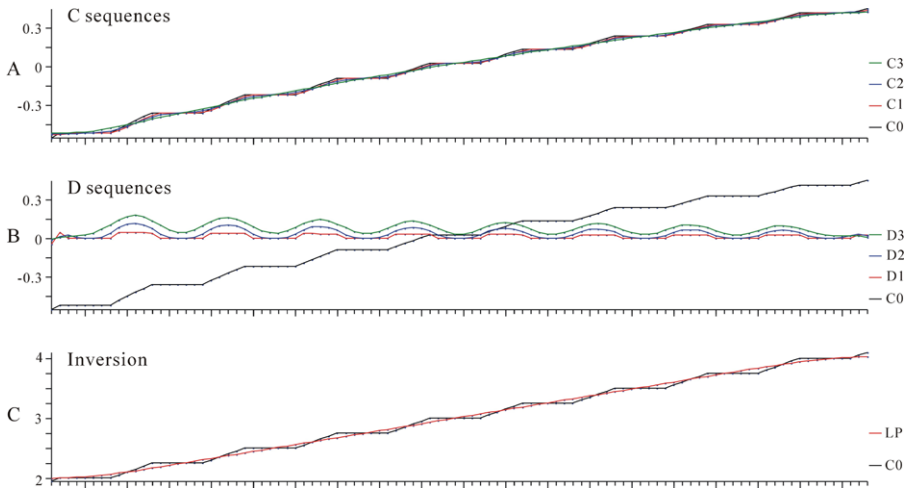


Fig. 3 Wavelet analyses of the logarithmic data of broadened anomalies in 1D model. **C** sequence = continuous sequence; **D** sequence = detailed sequence; **C0** = original data for wavelet analyses; **LP** = low-pass data of inversion

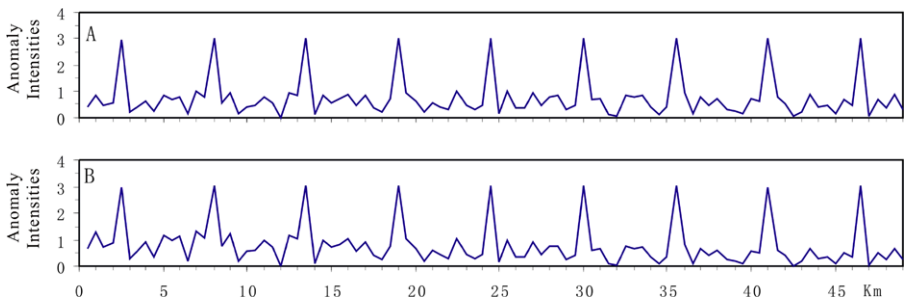


Fig. 4 Results of elimination of the influence of caprock thickness in 1D model (Fig. 1). **(A)** is the result from the correction of only anomalies; **(B)** from the correction of all the data including anomalies and background

where F_i ($i = 1, 2, 3, \dots, n$) is the correction factor for each sample; n is the number of samples; LP_i ($i = 1, 2, 3, \dots, n$) is the result of inverse log-normalization of low-pass filtering data as shown in Fig. 3C. The mean value in Eq. (1) is used to ensure the average value of the whole data does not change considerably after correction. The multiplication of F_i ($i = 1, 2, 3, \dots, n$) with the data of anomalies in Fig. 1 can accurately correct anomaly intensities and thus completely eliminate the influence of caprock thickness, as shown in Fig. 4A. In the case that the influence of caprock thickness is so weak that the anomalies can be separated from the background before eliminating the influence of caprock thickness, as shown in Fig. 1, this ideal effect can be achieved in this manner.

In practice, however, anomalies cannot be effectively separated from background where the influence of caprock thickness is too intense. Therefore, the correction factor cannot be simply used to multiply anomaly data. We multiply the correction

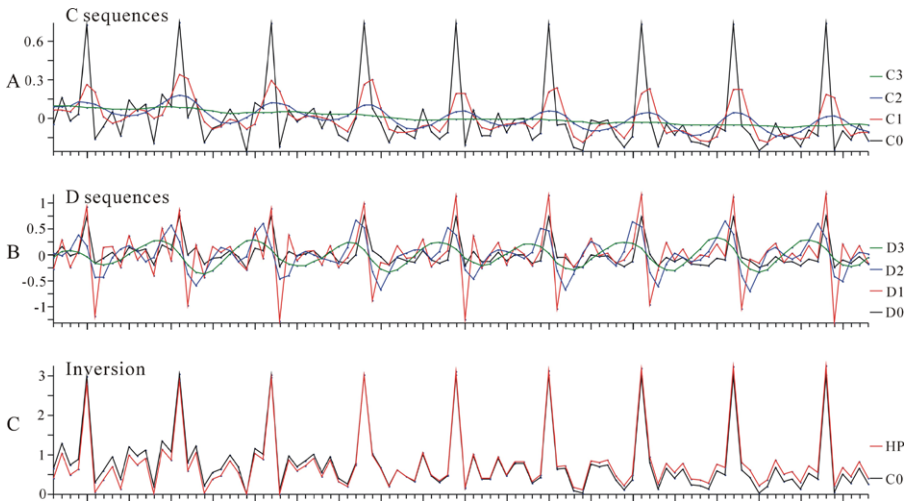


Fig. 5 Results of elimination of the interference introduced from multiplying correction factor and the whole data for eliminating influence of caprock thickness in 1D model. **HP** = results of high-pass filtering

factor with the whole data including anomalies and background. This multiplication must result in background variation (Fig. 4B): that is, importing interference (low-frequency information). This interference can also affect anomaly recognition and interpretation (Zhang and Liao 1998; Zhang et al. 2003, 2006). The imported interference can be eliminated in the same manner as elimination of surface interference of superimposition type with wavelet analysis (Zhang et al. 2003). The results of the elimination of this interference are shown in Figs. 5A, B and C. The background variation is greatly reduced. Compared with anomalies in Fig. 1, the anomalies shown by the results of high-pass filtering (HP in Fig. 5C) indicate that the influence of caprock thickness is greatly decreased. Although the intensities of anomalies of HP in Fig. 5C still vary, this small variation can be accepted for anomaly recognition (Zhang 1993; Zhang and Liao 1998; Zhang et al. 2003, 2006). In the case that this variation of anomaly intensities (corrected once) cannot be accepted, the low-pass filtering data corresponding to HP in Fig. 5C can be used as LP_i ($i = 1, 2, 3, \dots, n$) in Eq. (1) to calculate the correction factor for the second correction. In this way, the iterative corrections can be conducted until the variation of anomaly intensities becomes acceptable.

For the two-dimensional model (Fig. 2), a restriction condition for anomaly broadening is added. A broadened anomaly can cover only one original anomaly peak but does not cover the other peaks. In surface geochemical survey, the distances between anomalies are unknown. Therefore, anomaly peaks need to be judged in anomaly broadening. The broadening of an anomaly at one direction should stop when another peak is met. Figure 6 shows the data points of the broadened anomalies from the two-dimensional model in Fig. 2. After interpolation, extrapolation and border treatment, two-dimensional wavelet analysis was conducted, which was introduced in Zhang et al. (2003, 2006). The extraction of the information of caprock thickness influence is similar to the elimination of two-dimensional surface interference in

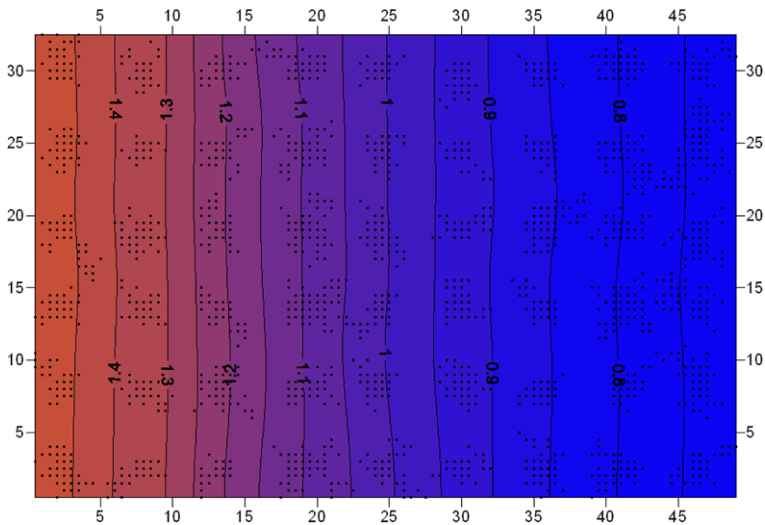


Fig. 6 Data points of the anomalies broadened from the 2D model and correction factor computed from the broadened anomalies with wavelet analysis at scale 3

most parts. The preprocessed data of broadened anomalies from the two-dimensional model were decomposed first in the survey line direction and then the decomposed data were further decomposed in the direction perpendicular to the survey lines. The inverse transformation of wavelet analysis was conducted first in the direction perpendicular to the survey lines and then in the survey line direction. Log-normalization and inverse log-normalization were carried out before and after the wavelet analysis, respectively. The correction factor for the two-dimensional model is calculated with Eq. (1) and LP_i ($i = 1, 2, 3, \dots, n$) obtained from the low-pass filtering at scale 3 of wavelet analysis. The correction factor gradually increases from right to left, whose distribution is contrary to the variation trend of anomaly intensities in Figs. 1 and 2. We multiplied this factor with the data of the two-dimensional model shown in Fig. 2. Then the interference imported from this multiplication was eliminated with two-dimensional wavelet analysis in the same manner as elimination of surface interference of superimposition type (Zhang et al. 2003). Figure 7 indicates that the anomalies are properly corrected via the elimination of caprock thickness interference and thus can be completely shown in the contour map.

In summary, the procedures for eliminating the influence of caprock thickness includes: (1) broadening anomalies, interpolating and extrapolating the data of the broadened anomalies; (2) log-normalization and border treatment; (3) with Mallat's wavelet, conducting wavelet analysis of these preprocessed data and taking the low-frequency information of intensity variation of anomalies via low-pass filtering; (4) calculating the correction factor with Eq. (1); (5) comparing the correction factor with geological data and affirming the validity of the correction factor; (6) multiplying the correction factor with original data influenced by caprock thickness if the correction factor is valid; (7) eliminating the interference imported from this multipli-

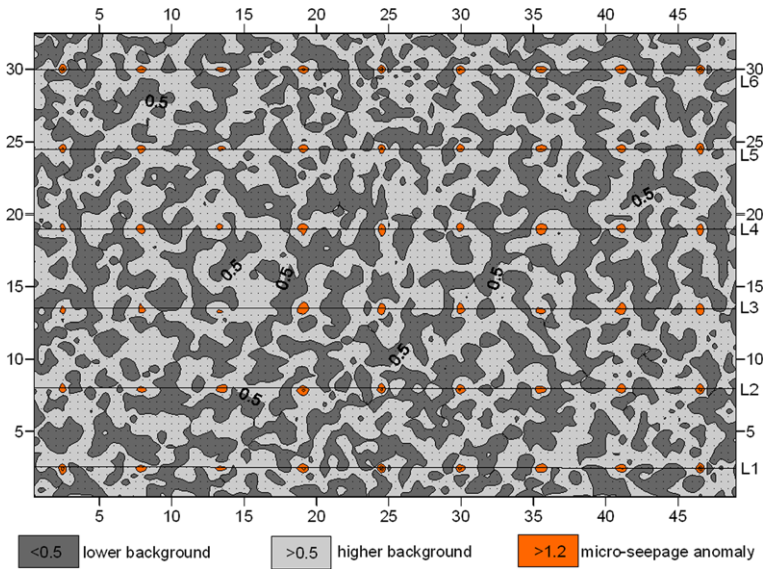


Fig. 7 The final result of the elimination of caprock thickness influence, in which the interference introduced from multiplying correction factor and all data were eliminated

cation in the same manner as elimination of surface interference of superimposition type; and (8) plotting the maps of the final result and affirm its rationality.

In a case where there is only one set of caprock with variable thickness, the burial depth of oil/gas pools may be correlative with the caprock thickness, as shown in the one-dimensional model (Fig. 1). In this scenario, the method for elimination of caprock thickness influence can be used as the method for elimination of the influence of burial depth on anomaly intensities and the correction factor can be used to predict burial depth of oil/gas pools.

4 Application

The study area lies in the southern slope of the Dongying Depression in East China (Fig. 8). The depression, one of the most petroliferous basins in East China, is a half-graben with a faulted northern margin. The source rocks are dark mudstones and shales in the upper part of the Sha-4 Member of the Paleogene Shahejie Formation (Es_4^U) and the lower part of the Sha-3 Member of the Paleogene Shahejie Formation (Es_3^L). Hydrocarbon migration and accumulation occurred twice: (1) at the end of the deposition of the Paleogene Dongying Formation overlying the Shahejie Formation, The source rocks in Es_4^U entered the oil window and began discharging hydrocarbons to reservoirs, but the amount of generated hydrocarbons was limited as hydrocarbon generation was disrupted with the uplifting and erosion caused by the Himalayan movement and; (2) from Neogene to Quaternary, with successive and overall subsidence, the deeply buried source rocks in both Es_4^U and Es_3^L were further matured with intensifying hydrocarbon generation and relatively high oil maturity (Zhu et al.

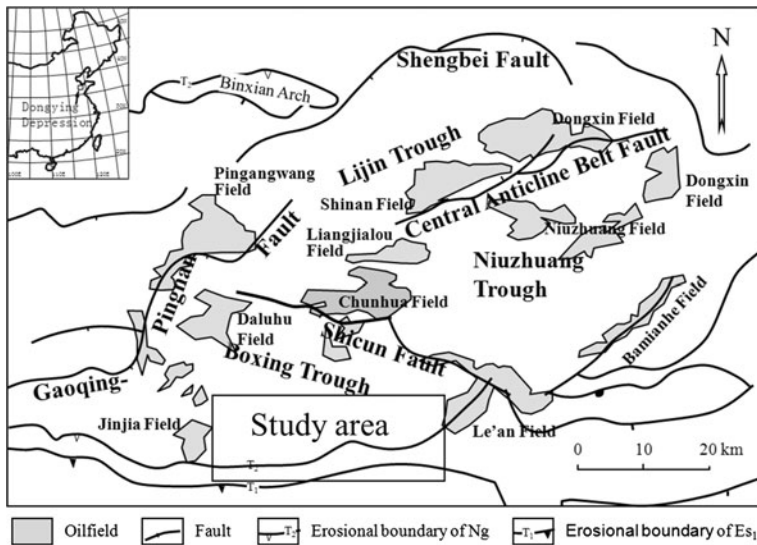


Fig. 8 Outline map of the Dingyong Depression, East China, showing oil fields and the study area (after Zhang et al. 2009, 2011). Ng = Neogene Guantao Formation; Es₁ = the Sha-1 Member of the Paleogene Shahejie Formation

2004). Faults, sandstones and unconformities are the major pathways of oil/gas migration. Several source-reservoir-seal assemblages are developed in the Kongdian and the overlying Shanhejie Formations (Zhang et al. 2009, 2011). In the study area, over 40 wells were drilled and six of them yielded commercial oil flow. The oils in this area are derived from the source kitchen in the Boxing trough in the south part of the depression (Fig. 8). The burial depth of reservoir rocks in the slope ranges from 2200 m in the north to 800 m in the south. In the study area, there are three main sets of caprocks in the Es₃, the Neogene Guantao (Ng) and Minghuazhen (Nm) Formations, respectively. The thickness of each set of caprock varies largely from 0 to more than 100 or 200 m. Thick caprocks are distributed in the northern part of this area with the thickest developed in the northwest (Fig. 9).

As part of a petroleum exploration program, a geochemical survey was conducted over the study area with a sampling grid of 0.5 × 0.5 km in 1998. 2080 soil samples were collected from the depth of 1.5 m. As most of the samples are sand and clayey sand, sand removal by sieving could not be applied to reduce the surface interference. The dry samples were briefly sieved with 40 meshes and analyzed using Horvitz's approach (Horvitz 1939, 1972, 1985) for acid-extractable hydrocarbons: CH₄, C₂H₆, C₃H₈, iC₄H₁₀, nC₄H₁₀, iC₅H₁₂, and nC₅H₁₂. Table 1 shows the minimum, mean and maximum values of the acid-extractable hydrocarbons in the study area. Meaningful anomalies of these hydrocarbons over or near oil pools have not been achieved with the methods for surface interference elimination and anomaly recognition (Zhang 1993; Zhang and Liao 1998, Zhang et al. 2003, 2006). In Fig. 10, the alternative distribution of higher background and lower background illustrates that the surface interference of acid-extractable propane was completely eliminated (Zhang et al. 2003). Nevertheless, there are no anomalies in the northwest part of the

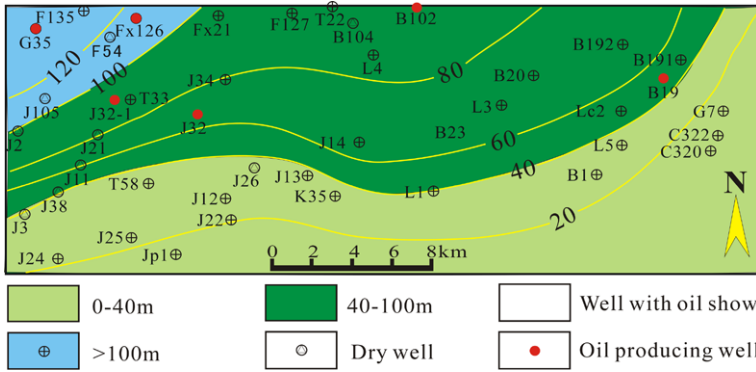


Fig. 9 Isopach map of caprocks in the Guantao Formation in the southern slope of the Dongying Depression

Table 1 Minimum, mean and maximum values of the acid-extractable hydrocarbons in the southern slope of the Dongying Depression

	CH ₄	C ₂ H ₆	C ₃ H ₈	iC ₄ H ₁₀	nC ₄ H ₁₀	iC ₅ H ₁₂	nC ₅ H ₁₂
Min	10.3	1.3	0.2	n.d.	n.d.	n.d.	n.d.
Mean	619.6	48.7	13.7	3.9	4.6	2.2	1.2
Max	4553.0	717.0	262.0	93.6	100.0	47.1	25.0

All values in ul/kg. n.d. = no data / below detection limits

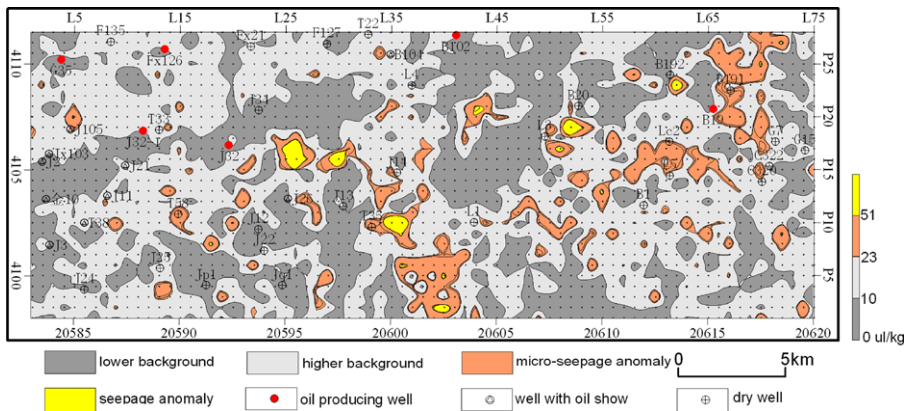


Fig. 10 Anomalies of acid-extractable propane after the elimination of surface interference in the southern slope of the Dongying Depression

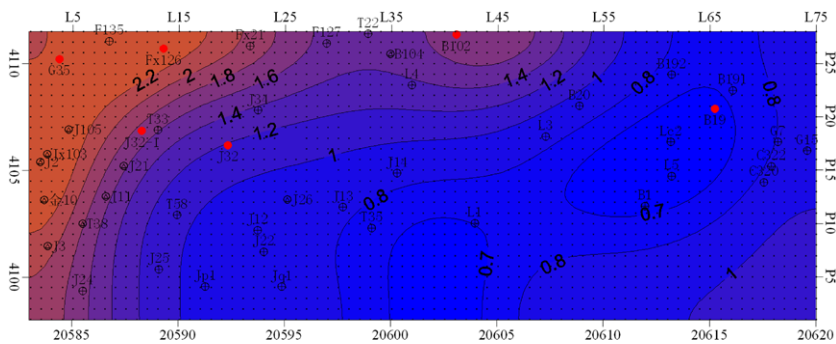


Fig. 11 Data points of the anomalies broadened from the acid-extractable propane in the southern slope of the Dongying Depression and correction factor computed from the broadened anomalies with wavelet analysis at scale 3. Refer to Fig. 9 for well legends

study area where most oil producing wells are located. The reason for this should not be the surface interference. The burial depth of reservoir rocks in the study area should not be the reason either, as it is shallow. Therefore, the influence of caprock thickness on anomaly intensities may be the reason for disappearance of anomalies in the northwest part.

To solve this problem, the newly developed method in this paper was applied to eliminate the influence of caprock thickness. Figure 11 shows the data points of the broadened anomalies from the data shown in Fig. 10 and the distribution of the correction factor computed by using Eq. (1). Generally, the correction factor is high in the NW part and decreases from NW to SE, which is corresponding to the features of caprock thickness variation. In the SE corner of the study area, however, the correction factor shows an increasing trend and is close to 1. In this corner, the caprock thickness is less than 20 m (Fig. 9). Such thin caprock may not effectively preserve oil. Therefore, the correction factor no longer decreases in the SE corner although the caprock thickness shows a decreasing trend from NW to SE. That may imply that the thickness for the effective caprock in the study area should be over 20 m. The correction factor was used to multiply the propane data after the surface interference elimination shown in Fig. 10. The interference imported from this multiplication was eliminated with the wavelet analysis. Figure 12 shows the final result of the elimination of caprock thickness influence on anomaly intensities. The anomalies in the NW part of the study area are enhanced and appear coincident with oil wells.

The data of acid-extractable CH_4 , C_2H_6 , iC_4H_{10} , nC_4H_{10} , iC_5H_{12} , and nC_5H_{12} were all processed in the same manner. These processed data were used to plot isoline maps by interpolation. Figure 12 is one of the univariate anomaly maps plotted with the anomaly recognition methods in Zhang (1993) and Zhang and Liao (1998). Although some noise appears in this map, it can be reduced when multivariate recognition is conducted (refer to Zhang and Liao 1998; Zhang and Bai 2002). The multivariate anomalies are studied elsewhere.

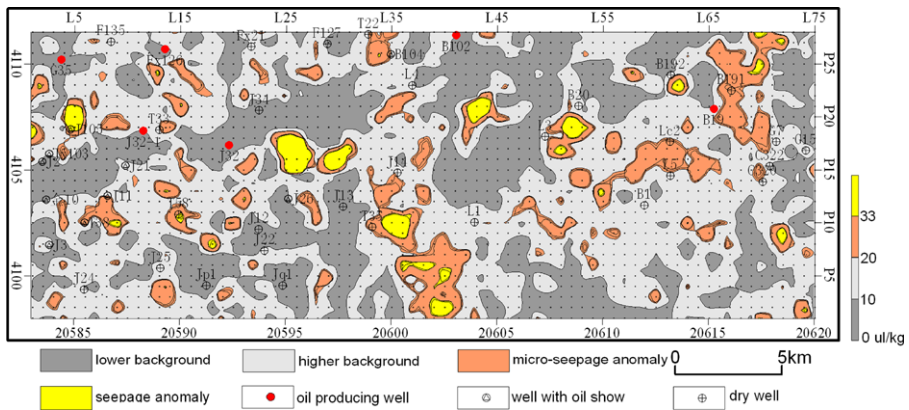


Fig. 12 Anomalies of acid-extractable propane after the elimination of both surface interference and caprock thickness influence in the southern slope of the Dongying Depression

5 Conclusions

Surface interference in geochemical exploration for hydrocarbons has been considered to be so noticeable that many researchers attempted to develop methods for its elimination. On the contrary, the influence of caprock thickness on anomaly intensities has been ignored in surface geochemical surveys. However, this paper has revealed that the influence can also lead to unreliable or inaccurate predictions where caprocks are either very thick or vary considerably in thickness. As surface interference elimination and anomaly recognition are not enough to get reliable anomalies in the case of intense influence of caprock thickness, the influence of caprock thickness must be eliminated.

The variation of caprock thickness provides low-frequency information in geochemical data. Therefore, the information of the influence of caprock thickness can be extracted via low-pass filtering with the wavelet analysis. The digital conceptual models of this influence, established in this paper on the basis of the features of anomalies and background, can help to analyze the digital characteristics of the influence. The method for eliminating the influence of caprock thickness was set up and tested on the basis of these models. The application of this method in the southern slope of the Dongying Depression illustrates that the method is effective to eliminate the influence of caprock thickness on anomaly intensities. Although this method is established at present for eliminating the influence of caprock thickness, we believe that it can be utilized to correct anomaly intensities whose variation arises from other geological influences providing low-frequency information and only changing anomaly intensities.

Acknowledgements We would like to express our gratitude to Messieurs Zhongxiang Cao, Kebin Zhao, Yongjin Gao and Changqing Sun of the Sinopec Corp. for their generous contribution of geological and geochemical data for this study. This research was financially supported by National Science and Technology Major Project of the Ministry of Science and Technology of China (No. 2008ZX05008-004-20).

References

- Abrams MA (1992) Geophysical and geochemical evidence for subsurface hydrocarbon leakage in the Bering Sea, Alaska. *Mar Petroleum Geol* 9:208–221
- Abrams MA (2005) Significance of hydrocarbon seepage relative to petroleum generation and entrapment. *Mar Petroleum Geol* 22:457–477
- Abrams MA, Dahdah NF (2010) Surface sediment gases as indicators of subsurface hydrocarbons—examining the record in laboratory and field studies. *Mar Petroleum Geol* 27:273–284
- Bolton EW, Maasch KA, Lilly JM (1995) A wavelet analysis of Plio-Pleistocene climate indicators: a new view of periodicity evolution. *Geophys Res Lett* 22(20):2753–2756
- Brown A (2000) Evaluation of possible gas microseepage mechanisms. *Am Assoc Pet Geol Bull* 84(11):1775–1789
- Burns KA, Greenwood PF, Summons RE, Brunskill GJ (2001) Vertical fluxes of hydrocarbons on the Northwest Shelf of Australia as estimated by a sediment trap study. *Org Geochem* 32:1241–1255
- Canet C, Prol-Ledesma RM, Escobar-Briones E, Mortera-Gutierrez C, Cruz RL-S, Linares C, Cienfuegos E, Morales-Puente P (2006) Mineralogical and geochemical characterization of hydrocarbon seep sediments from the Gulf of Mexico. *Mar Petroleum Geol* 23:605–619
- Davidson MJ (1994) On the acceptance and rejection of surface geochemical exploration. *Oil Gas J* 94(23):70–76
- Dembicki H Jr (2010) Recognizing and compensating for interference from the sediment's background organic matter and biodegradation during interpretation of biomarker data from seafloor hydrocarbon seeps: an example from the Marco Polo area seeps, Gulf of Mexico, USA. *Mar Petroleum Geol* 27:1936–1951
- Horvitz L (1939) On geochemical prospecting—I. *Geophysics* 4(2):210–229
- Horvitz L (1972) Vegetation and geochemical prospecting for petroleum. *Am Assoc Pet Geol Bull* 56(5):925–940
- Horvitz L (1985) Geochemical exploration for petroleum. *Science* 229(4716):821–827
- Klusman RW (1993) Soil gas and related methods for natural resource exploration. Wiley, New York, pp 1–112
- Klusman RW, Saeed MA (1996) A comparison of light hydrocarbon microseepage mechanisms. In: Schumacher D, Abrams MA (eds) Hydrocarbon migration and its near surface effects. AAPG memoir, vol 66. AAPG, Tulsa, pp 157–168
- Li J (1997) Wavelet analysis and signal processing—theory, application and software. Chongqing Publishing House, Chongqing, pp 1–325 (in Chinese)
- Logan GA, Jones AT, Kennard JM, Ryan GJ, Rollet N (2010) Australian offshore natural hydrocarbon seepage studies, a review and re-evaluation. *Mar Petroleum Geol* 27:26–45
- Loseth H, Gading M, Wensaas L (2009) Hydrocarbon leakage interpreted on seismic data. *Mar Petroleum Geol* 26:1304–1319
- Mallat S, Zhong S (1992) Characterization of signals from multiscale edges. *IEEE Trans Pattern Anal Mach Intell* 14(7):710–732
- Mani D, Patil DJ, Dayal AM (2011) Stable carbon isotope geochemistry of adsorbed alkane gases in near-surface soils of the Saurashtra Basin, India. *Chem Geol* 280:144–153
- O'Brien GW, Lawrence GM, Williams AK, Glenn K, Barrett AG, Lech M, Edwards DS, Cowley R, Boreham CJ, Summons RE (2005) Yampi Shelf, Browse Basin, North-West Shelf, Australia: a test-bed for constraining hydrocarbon migration and seepage rates using combinations of 2D and 3D seismic data and multiple, independent remote sensing technologies. *Mar Petroleum Geol* 22:517–549
- Palacios G, Beltrán J, Lacuesta R (2011) Multiresolution approaches for edge detection and classification based on discrete wavelet transform. In: Oikkonen H (ed) Discrete wavelet transforms: algorithms and applications. IN-TECH, Rijeka, pp 81–100
- Pinet N, Duchesne M, Lavoie D, Bolduc A, Long B (2008) Surface and subsurface signatures of gas seepage in the St. Lawrence Estuary (Canada): significance to hydrocarbon exploration. *Mar Petroleum Geol* 25:271–288
- Price LC (1986) A critical review and proposed model of surface geochemical exploration. In: Davison MJ (ed) Unconventional methods in exploration for petroleum and natural gas, vol IV. Southern Methodist University Press, Dallas, pp 245–290
- Pyrak-Nolte LJ, Nolte DD (1995) Wavelet analysis of velocity dispersion of elastic interface waves propagating along a fracture. *Geophys Res Lett* 22(11):1329–1332

- Rollet N, Logan GA, Kernnard JM, O'Brien PE, Jones AT, Sexton M (2006) Characterisation and correlation of active hydrocarbon seepage using geophysical data sets: an example from the tropical, carbonate Yampi Shelf, Northwest Australia. *Mar Petroleum Geol* 23:145–164
- Ruan T, Fei Q (1992) Exploration geochemistry for oil and gas. The Press of China University of Geosciences, Wuhan, pp 1–120 (in Chinese)
- Sassen R, Milkov AV, Roberts HH, Sweet ST, DeFreitas DA (2003) Geochemical evidence of rapid hydrocarbon venting from a sea floor-piercing mud diapir, Gulf of Mexico continental shelf. *Mar Geol* 198:319–329
- Saunders DF, Burson KR, Thompson K (1999) Model for hydrocarbon microseepage and related near-surface alternation. *Am Assoc Pet Geol Bull* 83(1):170–185
- Sechman H, Dzieniewicz M (2007) Influence of soil moisture on the results of surface geochemical survey applied to petroleum exploration. *J Pet Sci Eng* 56:267–282
- Sechman H, Dzieniewicz M (2011) The example of background determination and mathematical processing of data from surface geochemical survey for the purposes of petroleum exploration. *J Pet Sci Eng* 78:396–406
- Sechman H, Dzieniewicz M, Liszka B (2012) Soil gas composition above gas deposits and perspective structures of the Carpathian Foredeep, SE Poland. *Appl Geochem* 27:197–210
- Tedesco SA (1995) Surface geochemistry in petroleum exploration. Chapman & Hall, New York, pp 1–125
- Tokhmechi B, Memarian H, Rasouli V, Noubari HA, Moshiri B (2009) Fracture detection from water saturation log data using a Fourier-wavelet approach. *J Pet Sci Eng* 69:129–138
- Wenger LM, Isaksen GH (2002) Control of hydrocarbon seepage intensity on level of biodegradation in sea bottom sediments. *Org Geochem* 33:1277–1292
- Xu W (1993) Near-surface geochemical prospecting study on the southern slope of Dongying Depression. *Geophys Geochem Explor* 17(2):81–88 (in Chinese)
- Zhang L (1993) A primary study of the method for anomaly recognition in geochemical hydrocarbon exploration. In: The proceedings of the 2nd Chinese geo-chemical hydrocarbon symposium, pp 55–62
- Zhang L (2003) Vacuum desorption of light hydrocarbons adsorbed on soil particles: a new method in geochemical exploration for petroleum. *Am Assoc Pet Geol Bull* 87(1):89–97
- Zhang L, Bai G (2002) Application of the artificial neural network to multivariate anomaly recognition in geochemical exploration for hydrocarbons. *Geochem, Explor Environ Anal* 2:75–82
- Zhang L, Bai G, Xu Y (2003) A wavelet-analysis-based new approach for interference elimination in geochemical hydrocarbon exploration. *Math Geol* 35(8):939–952
- Zhang L, Bai G, Zhao K, Sun C (2006) Restudy of acid-extractable hydrocarbon data from surface geochemical survey in the Yimeng Uplift of the Ordos Basin, China: improvement of geochemical prospecting for hydrocarbons. *Mar Petroleum Geol* 23:529–542
- Zhang L, Liao Z (1998) A study of the method for the recognition of anomalies in geochemical hydrocarbon exploration. *J China Univ Geosci* 9:72–80
- Zhang L, Wang A, Jin Z (2011) Origins and fates of CO₂ in the Dongying Depression of the Bohai Bay Basin. *Energy Explor Exploit* 29(3):291–314
- Zhang L, Zhao Y, Jin Z, Bai G, Yang L (2009) Geochemical characteristics of rare earth elements in petroleum and their responses to mantle-derived fluid: an example from the Dongying Depression, East China. *Energy Explor Exploit* 27(1):47–68
- Zhu G, Jin Q, Dai J, Zhang S, Guo C, Zhang L, Li J (2004) A study on periods of hydrocarbon accumulation and distribution pattern of oil and gas pools in Dongying Depression. *Oil Gas Geol* 25(2):209–215 (in Chinese with English abstract)